Monitoring Bridge Scour by Fiber Bragg Grating Sensors

Yung-Bin Lin
National Center for Research on Earthquake Engineering, 200, Sec. 3, Hsinhai Rd., Taipei, Taiwan 106
yblin@ncree.gov.tw

Jin-Chong Chen and Kuo-Chun Chang
Department of Civil Engineering, National Taiwan University, Taipei, Taiwan 106
jinqochen@ntu.edu.tw ; ciekuo@ntu.edu.tw,

Jihn-Sung Lai
Hydrotech Research Institute, National Taiwan University, 158 Chow-Shan Rd., Taipei, Taiwan 106
jslai@hy.ntu.edu.tw

Scour is one of the major causes for bridge failure. Scour failures tend to occur suddenly and without prior warning or sign of distress to the structures. The real-time monitoring systems for bridge scour by using fiber Bragg grating (FBG) sensors have been developed and tested. This FBG scour-monitoring system developed can measure both the process of scouring and the variation of water level changing. Several testing runs in the laboratory have been conducted to demonstrate the applicability of the FBG system. The results show that it has the potential to apply the system to the real-time monitoring on bridge scouring in the field.

1. Introduction

As well known, scour is one of the major causes for bridge failure. During the scour, foundation material below the pier footing would be eroded, leaving the infrastructure such as bridge piers and abutments in unsafe or in danger of collapse, and occasionally results in loss of life. There are more than thousand bridges have collapsed over the last 30 years in the U.S. and 60% of the failures are due to scour[1]. This problem represents also a serious burden for the Far East countries such as Taiwan, Japan, and Korea…etc., owing to there are series typhoons and floods attacked in every summer or fall season. Scour failures tend to occur suddenly and without warning or sign of distress to the structures. The nature of the failure is often the complete collapse of the entire part of a bridge. There are 68 bridges are damaged by the scour problem in Taiwan from 1996 to 2001[2]. Scour at a bridge crossing a river can be classified as general scour, contraction scour, or local scour. Among them, the local scour is much more important that is generally caused by the interference of the piers and abutments with the flow and is characterized by the formation of scour holes at the bridge pier or abutment. Many efforts and resources have done in development and evaluation of scour detection and measurement instrumentation. However, the depth of the scour at the piers is not simple to measure or to monitor during the flood.

There exist many equations and measurement methods or monitoring systems such as sonar, radar, and time-domain reflectometry (TDR) to estimate and to predict the local scour depth of bridge foundations[3-21]. However, most of the available techniques for measuring or monitoring local scour depth have limited application. For example, both of sonar and radar are easily to install, but the results are, difficult to interpret especially when the water flow filled with mud and debris or rocks during the flood. In addition, this noise due to the turbid flow will also make these systems cannot be used to

real-time monitor the process of the local scour during the flood. Radar and sonar are usually applied only after the scour event, and indicates the final status of the sedimentation surrounding a pier[3-5]. Whereas the real scour depth during a flood is much important to the safety of the bridge. The TDR technique operates by generating an electromagnetic pulse and coupling it to a transmission line or cable[6-7]. The response signal as there is any varying current or potential will changed. However, as the cable lengths over a couple of hundred meters, attenuation and pulse will disperse the TDR signal and this disadvantage reduces the ability to discern subtle scour change. In addition, the electromagnetic environment also affects its corresponding results. A piezoelectric sensor consisting of a series of spatially separated piezo films provides incremental spatial resolution to track the entire scour cycle[8], but it is delicate and susceptible to damage by the muddy water and debris in the flood.

The scour depth monitoring system then faces to develop a real-time and needs more reliable methods to install in the riverbed during the flood. Moreover, the use of any scour formulas must ensure that the expressions are relevant to the characteristics including the flows, the channel parameters of different river, and the sediment of the site. The limits of use, assumptions, and inadequacies of the formulas should also be established before the estimation equations are applied. The recognition of possible aggradation and degradation of the riverbed lever in response to a disturbance to the channels is furthermore important in the prediction of channel changes.

2. FBG sensors

Fiber Bragg grating (FBG) sensors are highly attractive owing to their inherent wavelength response and their multiplexing capability for the distributive sensing network. In contrast to conventional resistance strain gauges, these sensors have electromagnetic interference immunity, lightweightness and small size, high temperature and radiation tolerance, flexibility, stability, and durability against harsh environments. In addition, FBG sensors are absolute, linear in response, as well as interrupt immune and of low insertion loss so that they can be multiplexed in a series of arrays along a single optical fiber. Furthermore, FBG sensors are developed for quasi-distributed or multi-point strain monitoring in both surface mounted and embedded sensing applications to provide local damage detection.

As well known, the Bragg phase-matching condition[22] determines the Bragg wavelength, λ_B, of a fiber grating. The wavelength shift $\Delta\lambda_B$ of a fiber Bragg grating sensor subjected to physical disturbance can be expressed as

$$\frac{\Delta \boldsymbol{l}_B}{\boldsymbol{l}_B} = (1 - p_e)\boldsymbol{e} + (\boldsymbol{a} + \boldsymbol{x})\Delta\mathrm{T} \qquad (1)$$

in which P_e, $\boldsymbol{e}$, $\boldsymbol{a}$, $\boldsymbol{x}$, and $\Delta\mathrm{T}$ is the effective photoelastic constant, axial strain, thermal expansion coefficient, thermal optic coefficient, and temperature shifts, respectively. These coefficients generally depend on the type of optical fibers and the wavelengths at which they are written and

measured. However, in sensor applications, the wavelength shifts induced by the variations of the doped materials in optical fiber can be treated as constants, compared to structure strain, because the measurements of the fractional Bragg wavelength variation induced by the different doped materials is small.

3. Experimental setup and test results

There are two local scour monitoring systems developed in this paper. The FBG monitoring system of model I, as shown in Fig. 1, uses the cantilever mechanism to measure the local scour depths during the flood. Three FBG sensors are surface mounted on a cantilever beam with different wavelength that is series array along a single optical fiber in this test. Similarly to the model I, FBG sensors are also series array along a single optical fiber in Model II, whereas herein, the FBG sensors are mounted on cantilever plates which located at different depth along a steel pile that can be fixed to the pier or the abutment as shown in Fig. 2. Notably, all the FBG sensors of model I and model II are carefully packaged to protect the sensors from flow damage during the test. There are three test programs including the current level of a flow, the local scour depth, and the height of riverbed sediment after a flood are arranged to demonstrate this FBG-model II monitoring system in the test.

When the current flows to the cantilever beam (Model I), the deformation strain from the bending moment will generated and this corresponding strain will be detected directly by the FBG sensors, as shown in Fig.1, when the FBG sensor emerges out the sediment during the flood erosion. The scour depth will be obtained directly from the responses of the different FBG wavelengths.

As illustrated in Table 1, obtained from the test results of model I, the local scour depth can be observed directly from the maximum strain of its corresponding FBG sensors. For example, as shown in Table 1 and Fig. 3, the FBG_1 has the largest bending moment strain than those of other FBG sensors since only the FBG_1 emerges out the sediment. It is obvious that the scour depth is now at the location of FBG_1. As the current flow continues erosion, the strain of FBG_2 and FBG_3 will gradually emerge out in turns and show the maximum response as illustrated in figures 4 and 5. Notably, the response of the scour depth is real-time monitored by the FBG sensors in the test. It is also observed that there are sine-wave noises like signals which are induced by the tremble vibration of the cantilever. This tremble vibration correlated with the variation of fluid characteristics due to the presence of soil particles suspended, air bubbles and fluid turbulence or the eddy current flowing.

For Model II, the test setup of the sink system with 3% slope is illustrated as shown in Fig. 6. The scour monitoring system, Model II, is settled in the sink to measure the process of flow level, sediment situation, and scour depth. When the water flows to the cantilever plate, the FBG sensor will contact and respond the water temperature firstly, as shown in Fig. 7. The wavelength shifts from the water temperature is 0.025nm which corresponding to about 2^{o}C different to the ambient temperature[2]. The running water impacted to the cantilever plate and forced the plate bending which will generate bending strain. The flow level of running water can be obtained from the wavelength shifts of FBG sensor as shown in Fig. 7. As well known the friction of the basin particles affects the current velocity

of the running water. Fig. 8 not only real-time reveals the levels of running water but it also shows the friction effects and responds the current flow velocity at each current layer. These results about the velocity and the acting strain which correlated to the twinkling flow rate would be useful to real-time calibrate and to evaluate the flooding potential in a flood.

For the scouring test, the FBG sensor is affected and responds the temperature of the water flow at first as mentioned. This responding temperature of water flow shifts the wavelength of FBG sensor herein at around 0.02 nm which corresponding to 1~2^{o}C as shown in Fig 9. As the flow submerges gradually and impacts on the FBG sensor element, the case_1, the bending moment of the cantilever plate will be induced by the current flow and it indicates the height of the flow as shown in Fig. 9. At about the 150th seconds of the test history, to simulate the riverbed sediment process, the fine sand is poured in the path of the sink in the case_2 and case_3. Herein, the case_2, the tremble vibration noise like signals are induced by the muddy drift and the fluid turbulence as mentioned in model I. It is also observed that the friction reaction of the flow increased from the response of wavelength shifts as the sediment rose. The steady state flow force acting on the cantilever plate will be decreased as the sand is poured continually into the sink. When the sand continually poured and deposited in the sink, the cantilever plate will be covered and there are not any force acting on the unit as shown in the case_3 of Fig. 9. It indicates that the deposited height of the sediment after a flood. Case_4 simulates and shows the scouring process during a flood as illustrated in Fig. 9. The signal resembles the process of flow level measurement as case_1, since the cantilever plate will emerge out the deposited sediment and it reveals the scouring depth during a flood.

4. Discussion and summary

Scour is one of the major causes for bridge failure. Scour failures tend to occur suddenly and without prior warning or sign of distress to the structures. Moreover, the pits of erosion tend to fill as soon as the flood begins to decrease, the following inspections and measures in the periods of dry weather or after a flood, cannot furnish indications on the real and maximum scour depth reached by erosion during the event of flood. The nature of the failure is mostly the complete collapse of the entire of a bridge. This scour problem represents a heavy crisis for Taiwan, since typhoons and floods attacked often in summer and fall season.

There are two real-time monitoring systems for bridge scour by using fiber Bragg grating (FBG) sensors have been developed and tested. This FBG scour-monitoring system developed can measure both the process of scouring and the variation of water level changing. Several testing runs in the laboratory have been conducted to demonstrate the applicability of the FBG system. The results show that it has the potential to apply the system to the real-time monitoring on bridge scouring in the field. However, the installation procedures and the protection of the FBG scour monitoring system from flood damage need more studied and improved, especially the impact forces of flood are huge and usually filled with drift stone and debris.

References

1. Shirole, A. M. and Holt, R.C. "Planning fir a comprehensive bridge safety assurance program," Transp. Res. Rec. 1290, Transportation Research Board, Washington, D.C., 1991, pp.137-142

2. Lin, Y.B., Lin, T.K., Kuo, Y.H., Wang, L. and Kuo-Chun Chang, "Application of FBG sensors to strain and temperature monitoring of full scale prestressed concrete bridges," Optical Fiber Sensors Conference Technical Digest, 2002. OFS 2002, 15th , 6-10 May 2002, pp. 211 -214

3. Gorin, S. R. and Haeni, F.P. "Use of surface-geophysical methods to asses reiverbaed scour at bridge piers," Water Resour. Investigations Rep. No. 88-4212, U.S. Geological Survey, Hartford, 1989

4. Mason, R.R., and Shepard, D.M. "Field performance of an acoustic scour-depth monitoring system," Proc., Fundamentals and Advancements in Hydr. Measurements and Experimentation, ASCE, 1994, pp.366-375

5. Hayes, D.C. and Drummind, F.E. "Use of fathometers and electrical-conductivity probes to monitor riverbed scour at bridges and piers," Water Resour. Investigations Rep. No. 88-4212, U.S. Geological Survey, Hartford, 1995

6. Dowding, C.H. and Pierce, C.E. "Use of time domain reflectometer to detect bridge scour and monitor pier movement," Prof., Symp. and Workshop on Time Domain Reflectometry in Envir., Infrastruct. and Mining Apllication, 1994, pp.579-587

7. Yankielun, N.E. and Zabilansky, L. "Laboratory investigation of time-domain reflectometry system for monitoring bridge scour," Journal of Hydraulic Engineering, 1999, pp. 1279-1284

8. Lagasse, P.F., Richardson, E.V., Shall, J.D. and Price, G. R. "Instrumentation measuring scour at bridge piers and abutments," NCHRP Rep. 396, Washington, D.C., 1997

9. Baglio, S., Faraci, C., Foti, E. and Musumeci, R. "Stereo vision for noninvasive dynamic measurements of the scour process around a circular cylinder in an oscillating flow," OCEANS 2000 MTS/IEEE Conference and Exhibition , Volume: 2, Sept. 2000, pp. 987 -992

10. Davidson, N.C., Hardy, M.S.A. and Forde, M.C. "Bridge scour assessment by impulse radar," Radar and Microwave Techniques for Non-Destructive Evalution, IEE Colloquium on , 20 Nov 1995, pp. 8/1 -8/8

11. Ram Babu, M., Sunder, V. and Narasimha Rao, S. "Measurement of sea bed scour around a pile-simplified instrumentation," Underwater Technology, 1998. Proceedings of the 1998 International Symposium on , 15-17 April 1998, pp. 334 -339

12. Babu, M.R., Sundar, V. and Rao, S.N. "Measurement of scour in cohesive soils around a vertical pile - simplified instrumentation and regression analysis," Oceanic Engineering, IEEE Journal of , Volume: 28 Issue: 1 , Jan. 2003, pp. 106 -116

13. Baglio, S. and Foti, E. "Non-invasive measurements to analyze sandy bed evolution under sea waves action," Instrumentation and Measurement, IEEE Transactions on , Volume: 52 Issue: 3 , June 2003, pp. 762 -770

14. DeVault, J.E. "Robotic system for underwater inspection of bridge piers," Instrumentation & Measurement Magazine, IEEE , Volume: 3 Issue: 3 , Sept. 2000, pp. 32 -37

15. Wen-Miin Tian "The application of side-scan sonar system in monitoring benthic artificial reefs," Underwater Technology, 1998. Proceedings of the 1998 International Symposium on , 15-17 April 1998, pp. 312 -316

16. Judge, J. and Forbes, D. "Measurements of Currents, Bottom Sediments and Seafloor Disturbance CASP," OCEANS , Volume: 19 , Sep 1987, pp. 975 -980

17. Drapeau, G., Forbes, D. and Boczar-Karakiewicz, B "Near-Bed Currents and Sediment Transport on the Inner Scotian Shelf During CASP," OCEANS , Volume: 19 , Sep 1987, pp. 981 -986

18. Cuevas, K.J., Buchanan, M.V. and Moss, D. “Utilizing side scan sonar as an artificial reef management tool,” Oceans '02 MTS/IEEE , Volume: 1 , 29-31 Oct. 2002, pp. 136 -140

19. Shiahn-wern Shyue “Preliminary study on the distribution of artificial reefs by using multibeam echo sounder,” OCEANS '98 Conference Proceedings , Volume: 2 , 28 Sept.-1 Oct. 1998, pp. 1144 -1148

20. Johnson, P.A. and Ayyub, B.M. “Incorporating uncertainty into bridge pier scour estimations.” Uncertainty Modeling and Analysis, 1993. Proceedings., Second International Sy mposium on , 25-28 April 1993, pp. 136 -140

21. De Falco, Fernando and Mele, Raffaele “The monitoring of bridges for scour by sonar and sedimetri,” NDT and E International Volume: 35, Issue: 2, March, 2002, pp. 117-123

22. Albert, J., Theriault, S., Bilodeau, F., Johnson, D.C., Hill, K.O., Sixt, P. and Rooks, M.J. “Minimization of phase errors in long fiber Bragg grating phase masks made using electron beam lithography,” Photonics Technology Letters, IEEE , Volume: 8 Issue: 10 , Oct. 1996, pp. 1334 -1336

Table 1 scouring strain

	case-1	case-2	Case-3
sensor-1	**71**	**33**	**33**
sensor-2	**60**	**49**	**106**
sensor-3	**9**	**8**	**163**

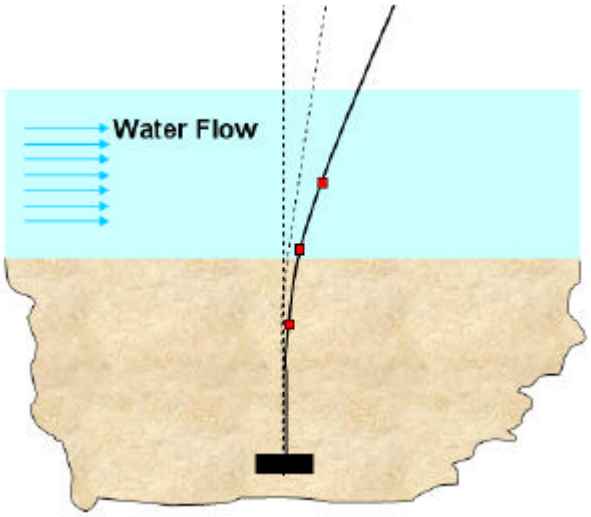

Fig. 1 The FBG scour monitoring system --Model I

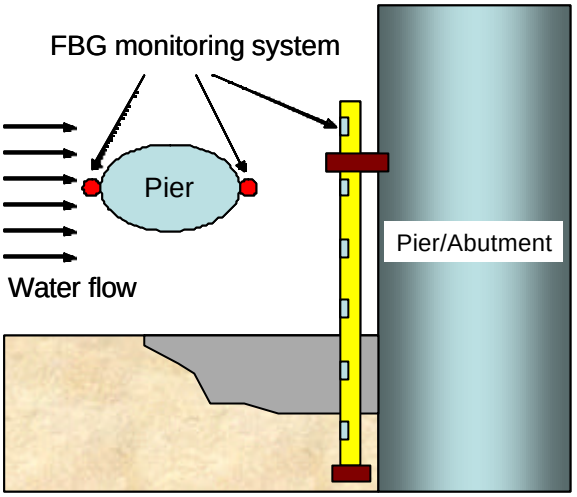

Fig. 2 The FBG scour monitoring system --Model II

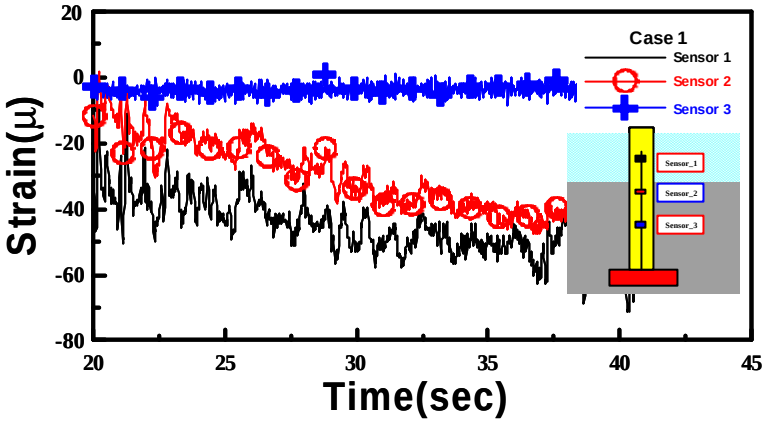

Fig. 3 Model I-- sensor_1 emerges out the sediment

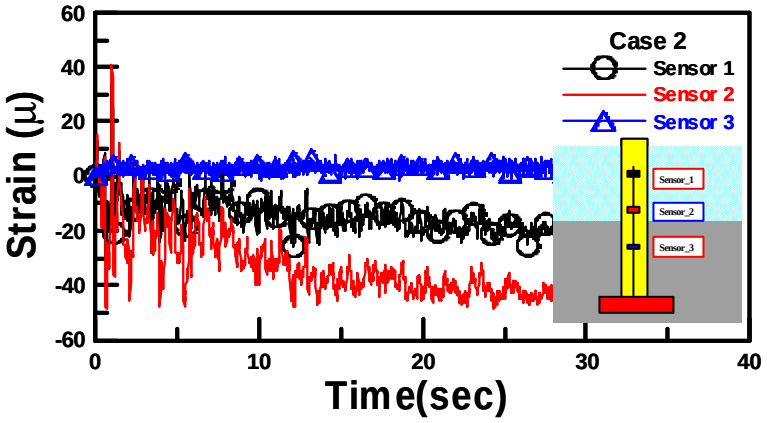

Fig. 4 Model I-- sensor_2 emerges out the sediment

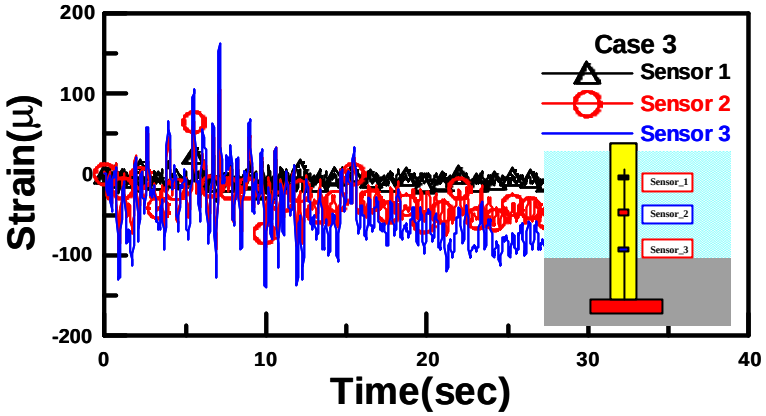

Fig. 5 Model I-- sensor_3 emerges out the sediment

Fig.6 The test setup of Model-II

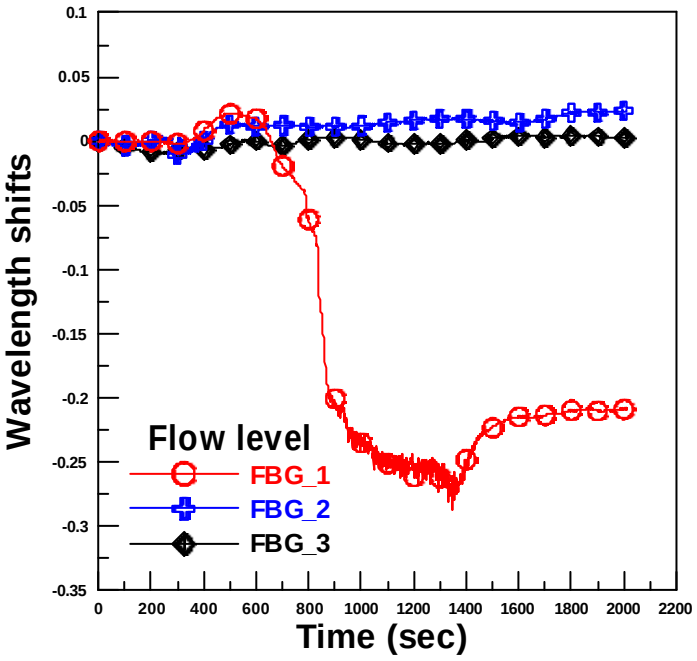

Fig.7 Test results of flow level __Model-II

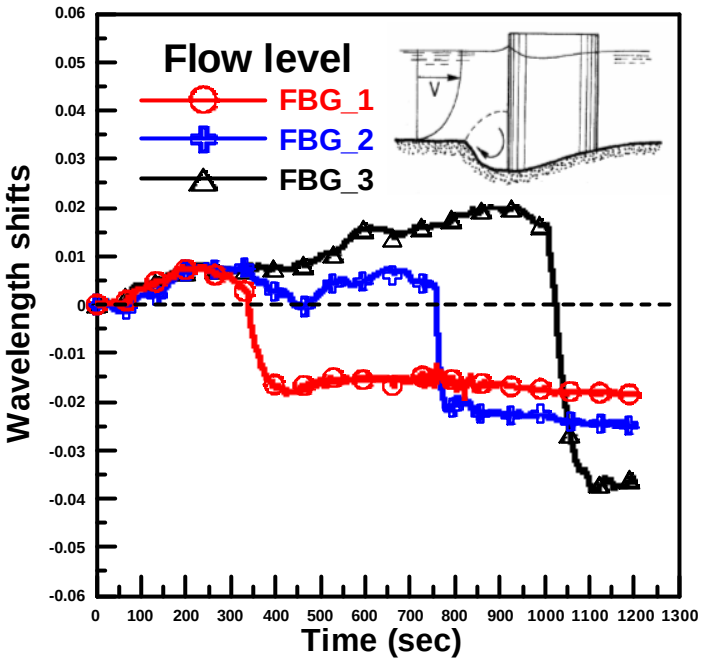

Fig.8 Test results of flow level __Model-II-case2

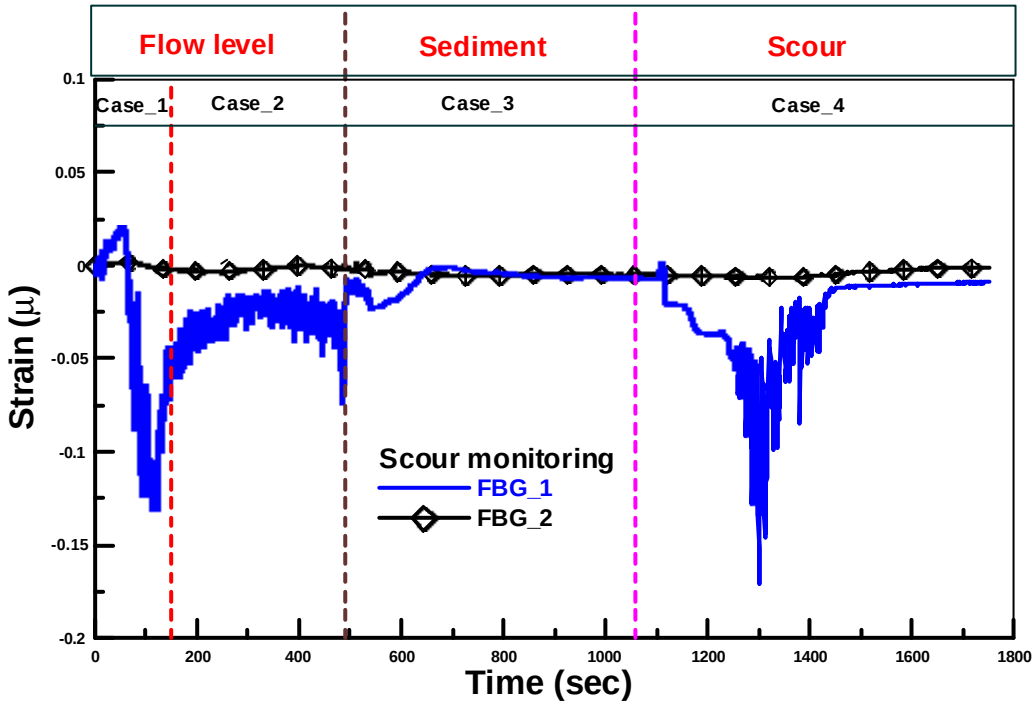

Fig. 9 Scouring test of Model II